Integrated Design Results for the MSR SRC Mars Ascent Vehicle

Darius Yaghoubi
Mail Stop EV71
4708 Apollo Street, Room 124F
Marshall Space Flight Center, AL 35812
darius.f.yaghoubi@nasa.gov

Shawn Maynor
Mail Stop EV43
4600 Rideout Road, Room 1425
Marshall Space Flight Center, AL 35812
shawn.b.maynor@nasa.gov

The primary mission of the NASA Mars Sample Return (MSR) Campaign is to return samples of the Martian surface to Earth for scientific study. As part of this campaign, NASA is developing a Mars Ascent Vehicle (MAV). This vehicle must survive an approximate two-year journey to the Martian surface as a payload aboard a separate lander spacecraft. After residing on the surface for another year, the MAV will carry a payload of samples into orbit. From there, following ejection from the MAV, the samples will rendezvous with an Earth return spacecraft for capture, and ultimately, return to Earth.

The design of the MAV represents a number of unique challenges, as no launch vehicle has ever left the surface of a planet other than Earth. Although conceptual designs for a MAV have been in various levels of development since the 1970s, none have achieved the level of fidelity and support that exists in the current MSR-MAV design. Early MSR-MAV concept studies examined multiple methods of propulsion, ultimately deciding that a Two-Stage-to-Orbit (TSTO) solid propulsion vehicle would provide the most capable performance in a Martian environment. Following this key architecture decision, the vehicle design was further matured to a Solid-Solid Guided-Guided (SSGG) architecture for NASA Key Decision Point A (KDP-A). Although the SSGG design was able to meet all mission constraints, concerns were raised regarding limited mass margin on other elements of the MSR campaign at such an early phase. A design challenge was issued to reduce MAV total mass by as much as possible. It was ultimately determined that by moving a number of components of the vehicle second stage to the first stage, the overall vehicle mass could be reduced significantly. The new design features a much smaller and completely unguided second stage.

This paper describes the resultant Solid-Solid Guided-Unguided (SSGU) MAV design concept developed as part of the Systems Requirement Cycle (SRC). This design was developed primarily by NASA Marshall Space Flight Center (MSFC), in association with NASA Jet Propulsion Laboratory (JPL) and NASA Langley Research Center (LaRC). The TSTO vehicle includes one solid rocket motor per stage. As the vehicle second stage is unguided, it features spin-stabilization to maintain vehicle stability during flight. An electromechanically actuated Thrust Vector Control (TVC) system and a monopropellant Reaction Control System (RCS) are employed for active guidance on the first stage. The vehicle is designed to deliver up to 0.47kg of Martian samples to a Mars circular orbit of 380km at 27° inclination. Due to the extremely unique design constraints of this mission, and a recent transition to a Risk Class A posture, the MAV team was compelled to devise unconventional solutions to the vehicle design. The detailed design and analysis of these subsystems and the vehicle as a whole are discussed in this paper relative to all of the engineering disciplines involved.

TABLE OF CONTENTS

1. INTRODUCTION

For decades, mankind has dreamt of studying one of Earth's closest galactic neighbors, Mars, in closer detail. Initially, this could only be done via observation through telescopes and the occasional meteorite of Martian composition. Although robotic capabilities, such as the Curiosity and Perseverance rovers, allow for significant scientific investigation, they are unable to replicate a human scientist in an Earth-based laboratory. Recent advances in technology, however, have made it possible to return samples of the Martian surface to Earth for scientific analysis. NASA, in partnership with the European Space Agency (ESA), aims to accomplish this task through the Mars Sample Return (MSR) campaign. This campaign includes the design and development of a Mars Ascent Vehicle (MAV). Although many iterations of a MAV with different key design drivers have existed in the past, each of them shares a common mission: to deliver a payload from the surface of Mars into orbit. The Systems Requirement Cycle (SRC) baseline version of this vehicle, being developed by NASA Marshall Space Flight Center (MSFC) in association with NASA Jet Propulsion Laboratory (JPL) is the most advanced MAV design to exist to date. As part of the MSR campaign, the MAV's primary mission is to transport samples of Martian geological and atmospheric composition into orbit, where they will be captured and returned to Earth.

The active component of the MSR campaign began in July 2020 with the launch of the Perseverance rover. After seven months in interstellar space, Perseverance landed in the Jezero Crater on Mars in February 2021. One of the primary missions of Perseverance is to use a robotic drill to collect surface and atmospheric samples from Mars and store them in small sample tubes. In 2028, MAV will be integrated with a Sample Retrieval Lander Spacecraft (SRL S/C) and launched from Earth. In a similar timeframe, a Sample Fetch Rover (SFR) and an Earth Return Orbiter (ERO) will also launch from Earth on separate vehicles. After approximately 33 months in interplanetary space, the SRL S/C will enter the Martian atmosphere and deploy the Mobile Lander Platform (MLP), with the MAV as its payload to land on the surface. The SFR will land on a separate lander. The SFR will conduct surface operations on Mars to collect the sample tubes left by the Perseverance rover and take them to the MLP. Perseverance itself also has this delivery capability. The MLP will use a Sample Transfer Arm (STA) to take the sample tubes from the SFR and place them into the payload compartment of the MAV, the Orbiting Sample (OS). The OS itself will be contained within a MAV Payload Assembly (MPA). The OS will be designed to hold up to 30 sample tubes of varying masses and densities. Once all sample tubes have been deposited in the OS, the OS and MPA will be closed and the MAV will be ready for flight. After being vertically ejected from the MLP, the MAV will ignite and begin its ascent to orbit. At the desired target orbit, the MAV will eject the OS, where it will rendezvous with the ERO, having already been in position above Mars. Once the OS has been captured, the ERO will return the samples to Earth to complete the MSR mission.

Conceptually, the MAV is a Two-Stage-to-Orbit (TSTO) launch vehicle. Each stage will have a Solid Rocket Motor (SRM) as the primary source of thrust, with the first stage having an independent electromechanically actuated Thrust Vector Control (TVC) system and the second stage being unguided and spin-stabilized. A monopropellant Reaction Control System (RCS) will be also be used for vehicle control, with a low shock actuator-based stage separation mechanism. Combined with the MPA and OS, the entire assembly creates the Mars Ascent System (MAS). A deconstructed view of the SRC exit configuration MAS is shown in Figure 1.

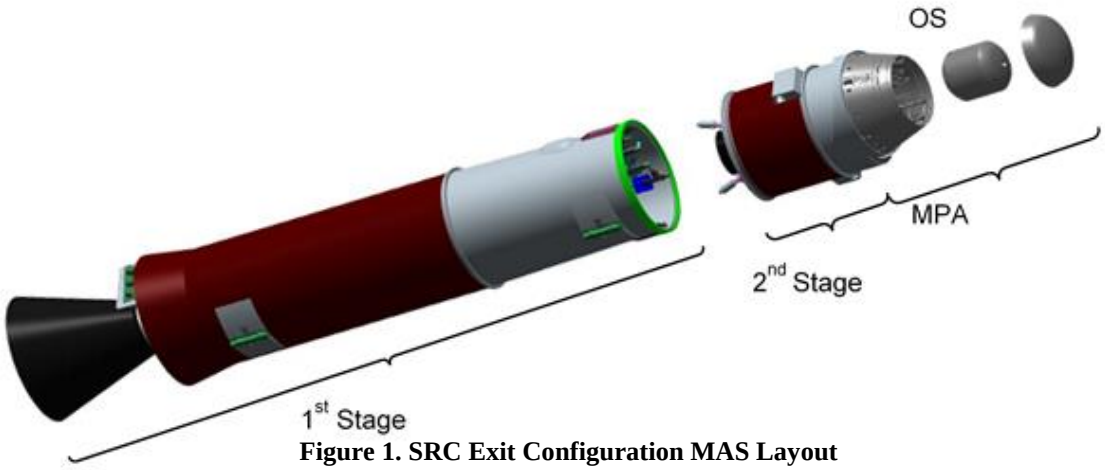

Figure 1. SRC Exit Configuration MAS Layout

2. SYSTEM REQUIREMENTS CYCLE

In Spring 2021, NASA completed the second analysis cycle for the MAV, the Systems Requirements Cycle (SRC). The primary purpose of this analysis cycle was to develop the system level requirements for the vehicle in preparation for the System Requirements Review (SRR), planned for November 2021. The first half of the SRC saw significant development of requirements at both the campaign and SRL levels. The growth of these requirements was extremely dependent on the capabilities of all MSR elements and payloads, including the MAV. Following the creation of these high-level requirements, the initial set of MAV system-level requirements were developed and matured. Although not the principal goal of the SRC, the technical fidelity of the vehicle design was also advanced. The initial technical advancement of the vehicle saw a number of both system-level and subsystem-level trade studies. These were vital for determining the vehicle overall configuration and architecture, some of which will be detailed throughout this paper. The SRC also saw a transition of the MAV mission as a whole to a NASA risk class designation of Class A, with tailoring [1]. This marks an increase in risk policy and compliance from the previous Class B+ designation, meaning stricter tolerances with items such as verification/validation, part selection, and fault tolerance.

Prior to the MAV SRC, alternative concept configurations were examined. In 2019, a Preliminary Architecture Assessment (PAA) was completed to determine whether a solid [2] or a hybrid [3] propulsion system would be most effective for the vehicle. Culminating in a decision package, the present solid concept was chosen going forward. Following the PAA decision package, the vehicle transitioned through NASA Key Decision Point A (KDP-A), as part of the Design Analysis Cycle-0.0 (DAC-0.0) [4]. This saw a departure from feasibility concept studies to an embrace of overall technology development. After the completion of DAC-0.0, a concern developed at the MSR level regarding the amount of mass margin available for the

SRL and MAV missions. Falling back on heritage Martian landers of similar size, such as those associated with the Curiosity and Perseverance rovers, it was observed that those programs had significantly higher mass margins at similar points in their design lifecycles. A design challenge was issued to reduce the mass of the SRL by as much as possible, including its MAV payload. Through a shortened analysis cycle, it was determined that as much as 125kg could be saved on the MAV design by moving as much mass as possible from the second stage to the first stage. This major architecture shift did have its downsides, however. Moving such a large amount of mass meant that the vehicle second stage would lose its guidance and control systems. It would in turn require spin-stabilization to complete its intended target insertion orbit. Although a challenge to design, the shortened analysis cycle found this concept to be feasible. The system architecture from there became known as the Solid-Solid Guided-Unguided (SSGU) concept and was carried forward as the starting point for the SRC.

Although the ultimate goal of the MAV is to deliver the Martian payload into orbit, there are additional design constraints to ensure that the vehicle meets the needs of the MSR campaign. These assumptions are as follows: hardware to be ready for a launch from Earth in 2028 to facilitate return of Martian samples in 2034; an aforementioned risk posture of Risk Class A, with tailoring; and a maximum MAV target mass allocation of 400kg with a geometric length not to exceed 2.99m and a diameter not to exceed 0.5m. The payload was defined as the total injected mass, including the MPA, OS, and expected 30 sample tubes, to the target Mars orbit. For the design and analyses completed in the SRC, this payload mass was assumed to be 16kg. A set of orbit constraints were also considered in order to accommodate rendezvous of the OS with the ERO. These included a nominal injection orbit of 380km, with an inclination angle of 27.3°, and a target orbit semi-major axis of 3776.2km. A lower bound periapsis of 300km was included.

The MAV ascent mission will begin with ejection from the MLP. This is performed by a pneumatically-activated Vertical Egress Controlled TipOff Rate (VECTOR) launch mechanism. This mechanism will ensure a complete physical separation between the SRL and MAV during first stage ignition. It directs all forces from ejection towards the Martian surface. A conceptual image of the MAV following VECTOR ejection is shown in Figure 2. Following ejection, the first stage Solid Rocket Motor (SRM1) will ignite and burn for approximately 70sec. After SRM1 burnout, the MAV will remain in a coast period for approximately 400sec. During this time, the MPA aerodynamic fairing and entire first stage will separate from the vehicle. After stage separation, the second stage will initiate a spin up via side mounted small scale SRMs. The entire second stage will be unguided and spin-stabilized at a rate of approximately 175 RPM. Having achieved the target spin rate, the second stage SRM, SRM2, will ignite and burn for approximately 18sec, raising the periapsis and circularizing the orbit. Following SRM2 burnout, the second stage will coast for up to 10 minutes while residual thrust from the SRM2 occurs. Side mounted small scale de-spin motors will then fire, reducing the spin rate to less than 40 RPM. Once the target orbit has been achieved, the MAV will command the MPA to eject the OS. The spent second stage of the MAV will remain in orbit, broadcasting a beacon signal for up to 25 days. This will aid in the capture of the OS by the ERO. This paper hereafter describes the individual subsystems associated with the SRC MAV design.

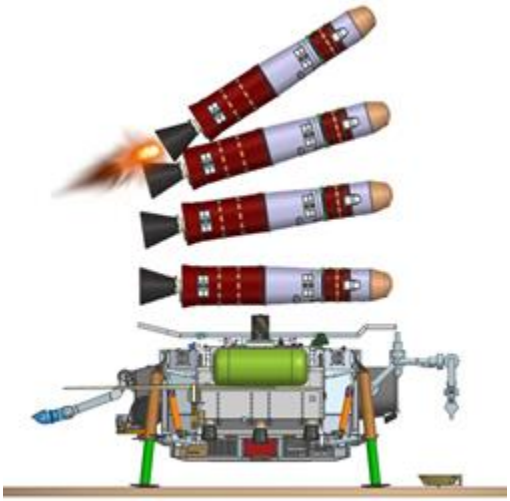

Figure 2. Conceptual VECTOR Ejection Trajectory

3. MAIN PROPULSION

Solid Rocket Motors

The MAV main propulsion system consists of two SRMs, each providing axial thrust to inject the payload into orbit. Each SRM features a carbon composite case. SRM1 features a trapped ball nozzle design with a Supersonic Split Line (SSSL) and an electromechanically actuated TVC system. SRM1 will carry the vehicle to a suborbital altitude prior to coast and stage separation. The second stage SRM, SRM2, does not feature a TVC system due to the SSGU design. It does, however, feature four small motors to provide the necessary spin and de-spin energy. Individual motor components such as the propellant grain have a high level of heritage as they have flown in Martian environments.

Initial sizing and optimization of each SRM began with designs from earlier analysis cycles. The previous DAC-0.0 configuration featured a total vehicle Gross Liftoff Mass (GLOM) of 525kg. The SRC configuration targeted a significantly reduced GLOM of 400kg, requiring smaller SRMs. An iterative process was employed, beginning with the DAC-0.0 motor designs scaled to the reduced GLOM. Early estimates of mass properties and orbital parameters were included in the iteration to further update the motor grain geometry. As the motors converged on a size, additional parameters were considered, such as thermal environments, motor case structural properties, and non-propulsive inert mass.

The motors themselves feature TP-H-3062 solid propellant. Various studies have shown that its Carboxy Terminated Polybutadiene (CTPB) binder is very capable of maintaining a reliable burn rate in extreme temperatures. This solid propellant has a high level of heritage, having been used in the descent stages of prior Mars missions such as Mars Exploration Rovers Spirit and Opportunity as well as Mars Pathfinder. The SRC propulsion design features 213kg of propellant for SRM1 and 47kg of propellant for SRM2. Each SRM is shown in Figure 3, including other elements of their respective stages.

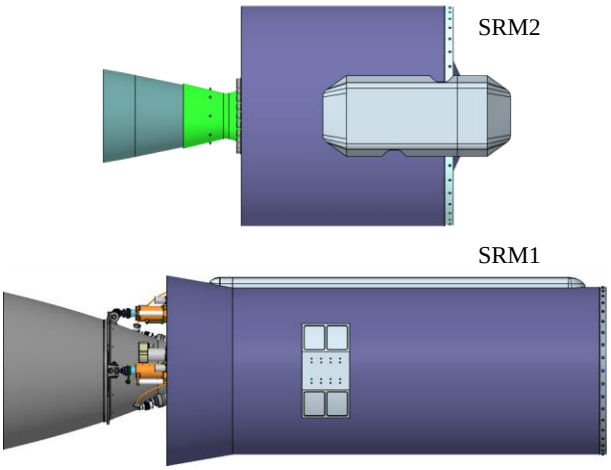

Figure 3. Solid Rocket Motors

Part of the SRM design and analysis included refinement and optimization of each nozzle. This was mostly applicable to SRM1, as loads induced on the nozzle structure are increased due to TVC gimbal during ascent. Computational Fluid Dynamics (CFD) simulations were performed with nozzles in a neutral position. Internal surface pressures were then converted to lateral and axial force vectors to further determine expected nozzle loads, with the structural design updated accordingly. This is shown in Figure 4. CFD results were also used to refine the TVC design by providing fluid-induced nozzle loads. This was crucial for sizing of TVC hardware such as electromechanical actuators. This is discussed further in Section 5. Transient gimballing simulations did not indicate a non-linear dynamic gimbal response.

Thermal environments were assessed for the development of each SRM. Throughout the mission lifecycle, each SRM will be exposed to a wide range of temperatures, including cold temperatures on the Martian surface, mild temperatures while on Earth, and high temperatures during actual motor burn. It is imperative that these thermal cycles do not introduce any propellant cracking or other flaws due to asymmetric thermal expansion. A thermal analysis was conducted to identify maximum expected temperature gradients across each SRM due to mission environments.

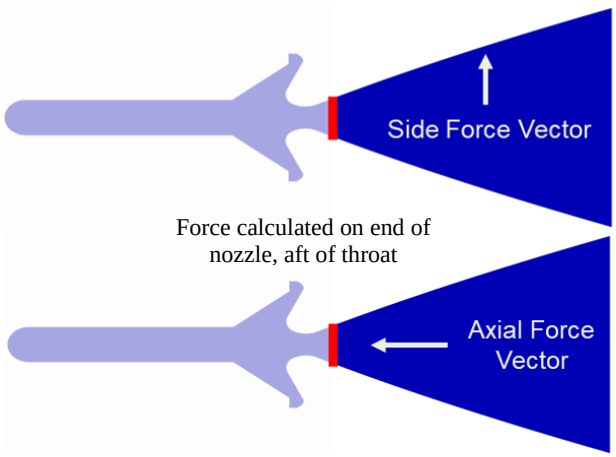

Figure 4. Nozzle Force Vectors

This analysis took into account both ambient and induced temperatures. SRM case thickness and insulation were sized accordingly to passively support desired temperatures. Active thermal conditioning will be maintained through heaters as described in Section 7.

One of the unique aspects of the MAV mission is that the vehicle itself is a payload aboard the SRL prior to its ascent mission. This requires it to be stored in a lateral position during major loads events such as Earth launch and Martian Entry, Descent, and Landing (EDL). The primary load path of the vehicle during these times passes directly through SRM1 and the interstage. The SRM1 case is designed to be load-bearing, with the SRL physical interface points located approximately halfway between nozzle tip and forward dome.

Spin & De-Spin Motors

Due to the lack of guidance during MAV second stage flight, the vehicle will enter a stabilized spin state prior to ignition of SRM2. This is achieved through the ignition of two small-scale SRMs mounted tangentially to the outer case of SRM2. These spin motors will fire directly following stage separation. The resultant spin state will resist the effects of external disturbance torques on the pitch and yaw planes of the MAV second stage. Following SRM2 burnout, a second pair of de-spin motors will fire to reduce the spin state to zero. Each spin and de-spin motor feature an aft closure with its nozzle canted 90°. The motors are attached to SRM2 via flange joints with case-integrated structural components. The motors are axially positioned relative to the stage 2 Center of Gravity (CG) so as to not impart unwanted lateral rotation on the vehicle. It is crucial that each pair of motors operates with as close to identical burn characteristics as possible; once the vehicle second stage has separated from the first stage, there will be no way to correct any unwanted motion. The spin and de-spin motors will undergo a series of tests and inspections to ensure that factors such as Propellant Bulk Mean Temperature (PMBT) and manufacturing tolerances do not negatively impact their performance and reliability. Although the case dimensions of the spin motors are similar to that of the de-spin motors, the actual propellant mass of the de-spin

motors is lower. This accounts for the reduced axial moment of inertia following SRM2 burn. Figure 3 shows the location of the spin and de-spin motors on SRM2 within an aerodynamic housing. Figure 5 shows the orientation of one pair of spin and de-spin motors with this housing removed. The L-shaped elements in the figure represent two pyrotechnic igniters per motor.

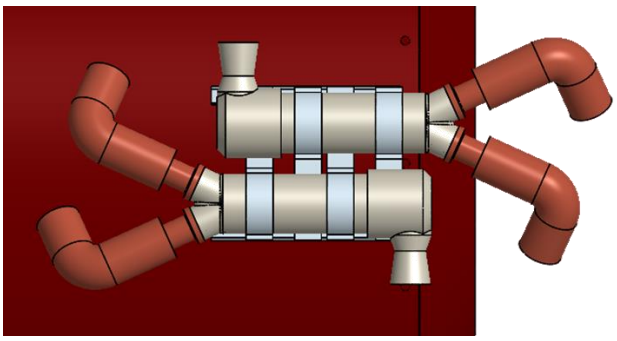

Figure 5. Spin & De-Spin Motors on SRM2

4. Reaction Control System

The MAV RCS provides attitude control about the vehicle roll axis during SRM1 burn. It provides full 3-axis control during coast. As the vehicle second stage is unguided, no RCS hardware exists on the vehicle following stage separation. This introduces a unique design constraint, as the RCS must be located entirely on the vehicle first stage. Ideally, the RCS thrust application point would be located as far from the vehicle CG as possible. This would maximize the moment arm, allowing for the least amount of thrust necessary to rotate the vehicle, increasing overall controllability. For the MAV SRC configuration, the only placement option for the RCS was on the interstage section of the first stage. It is located between the primary avionics and SRM2, as shown in Figure 6. Although not a concern for roll control, this placement creates a significantly reduced pitch and yaw moment arm over previous design configurations. The decreased controllability associated with this updated moment arm is described further in Section 10.

Sizing of RCS hardware was based upon the aforementioned controllability analysis. The RCS itself features a traditional 2-to-1 blowdown monopropellant architecture, leveraging existing Commercial-Off-The-Shelf (COTS) components where available. Hydrazine was selected as the propellant due to its extensive heritage and low density. Due to the unique mission, a customized propellant tank will be necessary. Originally, additive manufacturing was considered for the fabrication of this tank, however, recent changes in the overall MAV design found that traditional forging would be more appropriate. The tank features an elastomeric diaphragm to minimize ullage within the tank and reduce propellant slosh. Gaseous nitrogen will be used as the blowdown pressurant. The RCS features six individual lateral thrusters. Due to packaging constraints, the RCS frame is unaligned with the vehicle body frame, clocking the thrusters at an angle from the pitch and yaw axes.

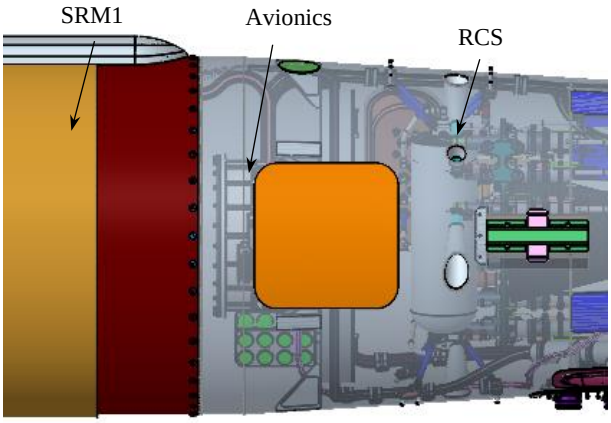

Figure 6. RCS Location

The nozzles are scarfed to prevent unwanted aerodynamic torques due to Outer Mold Line (OML) protuberances. The thrusters were assumed to be Aerojet Rocketdyne MR-111G thrusters, providing up to 5N of thrust each [5]. The actual thrusters used in the final design may vary. Figure 7 displays the overall RCS layout.

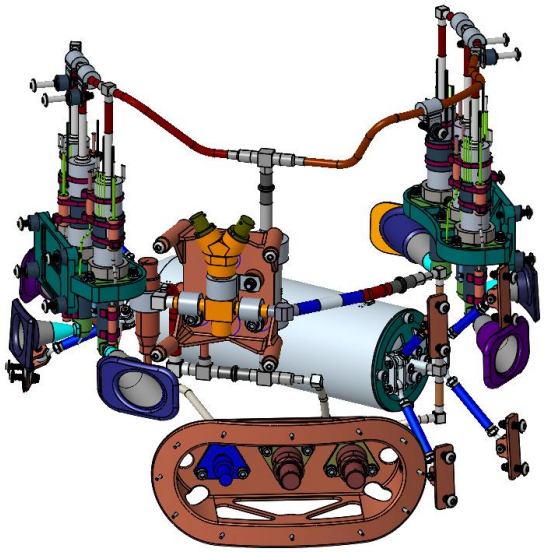

Figure 7. RCS Layout

Additional RCS hardware includes catalyst beds, various valves for operation and service, and heaters. Hydrazine freezes at 2°C, which is a significantly higher temperature than the vehicle expected minimum temperature of -40°C. This necessitates specialized heaters for the wetted RCS components to ensure that they do not freeze. Prior to launch from Mars, the RCS thruster valves and catalyst beds will be brought up to their operational set points. A null burn will be performed shortly after VECTOR ejection bring the catalyst bed to the correct thermal state. The supply lines of the RCS will be unheated until day of launch. The RCS thermal design is discussed in more detail in Section 7.

5. Thrust Vector Control

The MAV TVC system controls the vehicle about pitch and yaw planes during motor burn. It achieves this by adjusting the nozzle gimbal angle of the SRM1 to achieve a desired

thrust vector. Due to the unguided second stage, the TVC system only controls the vehicle during first stage burn. The MAV TVC system is mounted to the aft end of SRM1. It consists of a pyro-activated thermal battery, a Field-Programmable Gate Array (FPGA) firmware-operated controller, and two traditional electromechanical actuators clocked 90 degrees apart. Commands to the TVC controller are sent from the flight computer following interpretation of external disturbance torques. The two TVC actuators are attached to the stationary portion of the SRM1 case and to the gimballed SRM nozzle. These actuators were sized to gimbal the nozzle while under expected mission propulsive loads described in Section 3 and ascent loads described in Section 6. Figure 8 displays the actuators in respect to the SRM and nozzle. Note that the thermal battery and controller are not shown in this image as they are obscured by the nozzle itself.

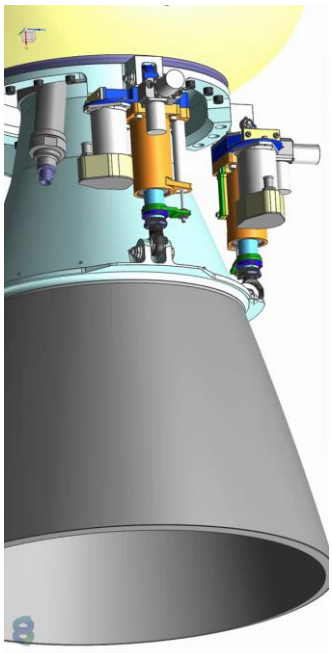

Figure 8. MAV TVC

The nozzle gimbal features a SSSL with a trapped ball design. This features a number of unique mission-specific advantages over a traditional elastomeric design. The internal geometry of a typical SSSL is shown in Figure 9.

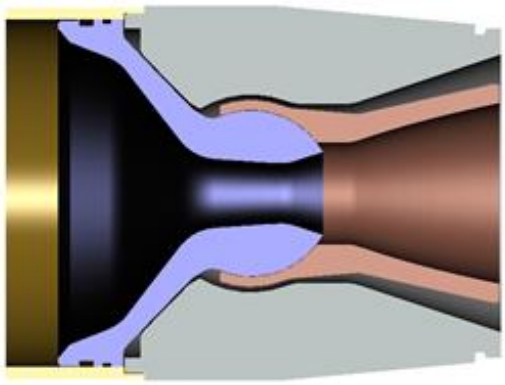

Figure 9. Example Supersonic Split Line

Elastomerics are known to become extremely brittle in cold temperatures and would likely perform poorly in a Martian environment. The actual joint of the nozzle is located downstream of the nozzle throat, allowing it to be unaffected by the high-pressure combustion environment. This decreases overall throat erosion. The specific SSSL architecture for the MAV imparts less normal force on nozzle bearings and seals, resulting in a significant reduction in friction. This decreases overall actuator mass and power draw. Shockwaves reflecting from the internal nose tip augment the mechanical deflection, decreasing the system's time constant and reducing overall packaging volume. The internal geometry of the trapped ball also leads to less penetration of heated aluminum oxide particles downstream of the throat.

A pyro-activated thermal battery provides the power necessary for operation of the TVC. Although thermal batteries have high heritage in Martian environments, they are limited in application as they are one-time-use power sources. Several demonstrations of end-to-end TVC operation and dynamic performance are necessary prior to MAV launch. Since the power for these TVC gimbal tests cannot be provided directly by the thermal batteries, all testing following Earth launch will be powered directly through primary avionics, described in Section 8.

The thermal battery in this design was sized to accommodate the maximum actuator duty cycle. It is likely that there will be excess power from the thermal battery for a portion of first stage flight. A trade study was conducted to determine if this power could be utilized in other MAV systems, such as RCS and pyrotechnics. The aim of the study was to reduce MAV battery quantities and thereby overall vehicle mass. Ultimately, the complexities involved in distributing power from the aft end of the vehicle to the primary avionics were found to add an unreasonable amount of mass, negating the need for such a design change.

6. STRUCTURES AND DYNAMICS

Loads & Dynamics

As mentioned in Section 3, the MAV loads environment is atypical for a launch vehicle in that it must withstand its maximum loads in a lateral direction while stored within the MLP during Mars EDL. This is contrary to a standard axial loads direction during ascent. As mentioned in Section 3, SRM1 contains one component of the primary load path for the vehicle. The vehicle interstage also contains a primary load path. These are both transferred from the MLP through the VECTOR attach points. Aside from these, the rest of the integrated vehicle is still expected to undergo significant structural loads throughout the mission. A loads analysis was performed to characterize these loads on the integrated vehicle to ensure structural capability. This analysis focused on two major groups of the mission, using differing methodology for each. The first group investigated quasi-static loads during Earth Ascent and Mars EDL. The second group investigated dynamic loads during VECTOR ejection and Mars ascent. Aside from the SRMs, the vehicle

interstage, forward structure, and separation mechanism provide loading capability. The interstage and forward structure were designed to be of an aluminum alloy material, machined with monocoque construction from simple ring forgings. Figure 10 displays the difference in loading hardware between propulsion and structural components, with orange representing structural elements and red representing propulsive elements. VECTOR attach points on SRM1 and the interstage are also shown.

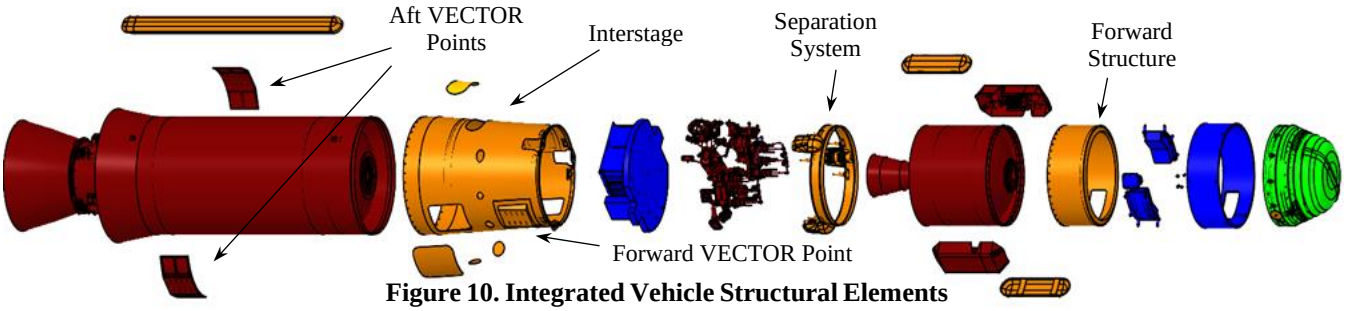

Figure 10. Integrated Vehicle Structural Elements

A single Finite Element Model (FEM) was developed for the processing of Earth launch and Mars EDL. Primary section loads (shears, moments, and P_{EQ}) were developed at 20 stations along the length of the vehicle, based on interfaces between sub-elements, changes to shape or thickness of the OML or Inner Mold Line (IML), merging/diverging of internal or external structures, and regular centerlines throughout the vehicle. Only 12 stations are visually distinct due to many stations overlapping at different interfaces. Figure 11 shows the Earth launch and Mars EDL FEM with annotated centerline stations implemented in the reduced models. These loads were developed using quasi-static modelling. For all quasi-static loads calculations, the vehicle was constrained at the vehicle interfaces with the MLP. All constraints were "pinned" in that they were constrained in the translational directions while being free to rotate. The constrained MAV FEM was then subjected to 11 different cases: 1g gravity loads in each axis, as well as 1 rotation/sec and 1 rotation/sec^2 clockwise and counter-clockwise about the CG of the MLP in in-plane axes. The loads from each gravity or rotational case were summed via superposition as required for each individual extreme in each regime. In total, 88 cases were considered from Earth launch to Mars landing.

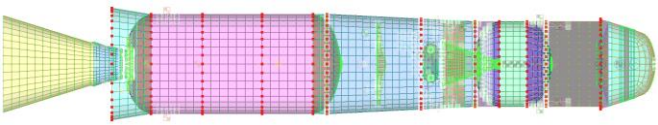

Figure 11. Earth Launch and Mars EDL FEM Mesh

A series of FEMs were created for development of the SRC MAV loads based off the model for VECTOR ejection and Mars ascent. Models were created as NASTRAN input data deck files and also in Craig-Bampton (CB) reduced form. The CB models were provided with force transformation matrices and output transformation matrices, for use in loads analysis. Each FEM represented one of ten different points in the MAV's ascent trajectory. The MAV SRC Mars ascent configuration yielded a structure with significantly higher natural frequencies than typically encountered during launch vehicle loads analysis, due to its relatively small size. Additional models incorporated into the loads cycle include aerodynamic line loads, buffet forcing functions, and trajectory loads. Envelopes were generated for section loads, distributed acceleration, acceleration at CG, distributed elastic displacement, interface forces, and equivalent forces. Figure 12 displays a sample axial loads envelope during Mars ascent. As expected, the primary axial loads during ascent are due to thrust from each SRM, with largest loading felt on SRM2. Lateral loads were largest during VECTOR ejection and RCS burns while in coast.

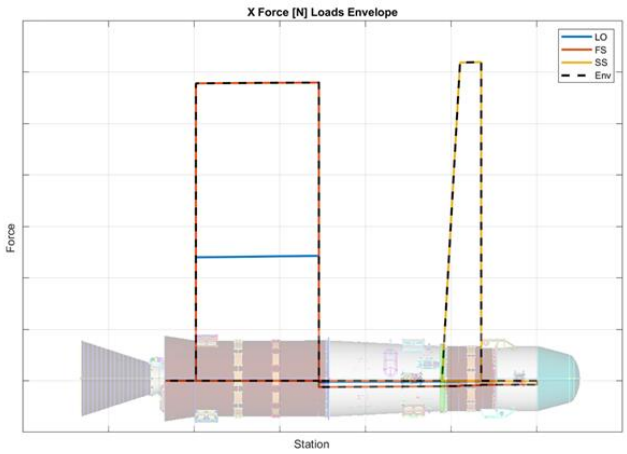

Figure 12. Sample Ascent Loads Envelope

Stage Separation Mechanism

The SRC MAV design features a number of mechanisms, particularly components such as pyrotechnics, stage separation, and the aforementioned TVC actuators. The stage separation mechanism is of particular interest for the MAV design. As with other structural components, it must withstand maximum loads in a lateral direction rather than axial. Industry standard stage separation mechanisms for vehicles of this size are not designed with lateral loads in mind. Even neglecting the lack of heritage in a Martian environment, previous studies have found stage separation faults to be the second most leading cause of US launch vehicle failures in the past 30 years [6]. In addition, due to the unguided MAV second stage, MAV trajectory and orbital performance is extremely sensitive to tip-off rates and vehicle pointing error during staging.

Due to the importance of the stage mechanism for mission success, a trade study was performed to examine available options and to identify forward work to ensure survivability and reliability. Prior to SRC, a clamp band-based mechanism was assumed. Although the idea of a clamp band mechanism was retained, part of the trade study involved increasing the fidelity of the design in its application to the SSGU vehicle. Outside of the clamp band mechanism, a Non-Explosive Actuator (NEA) system was studied as well as a Low-Shock Separation Nut (LSSN) system. As the name implies, a clamp band mechanism features a ring circumferentially clamped around the vehicle stages. Pyrotechnic devices would be used to sever the band. The NEA system, perhaps the simplest in design, features a series of springs used to actuate the separation without the use of pyrotechnics. The LSSN system features dual-initiated igniters contained within a series of pressure cartridges. As pressure fills the interior of the cartridge, a piston/cylinder/sleeve assembly is pushed forward, unlocking a threaded nut and releasing a bolt.

The first part of the trade study involved an analysis of each system's GNC performance and impacts on orbital behavior. Nominal performance of each did not reveal a key advantage for one over the other. Dispersed performance, however, found that the LSSN had the more favorable orbital performance. Additionally, it was found that the NEA system had a large contribution to tipoff rates due to simultaneity variance in individual springs. This is demonstrated in Figure 13. The reduction in pointing accuracy from this variance led to its removal from the trade study. The entirety of the GNC portion of trade is examined in more detail in Section 10.

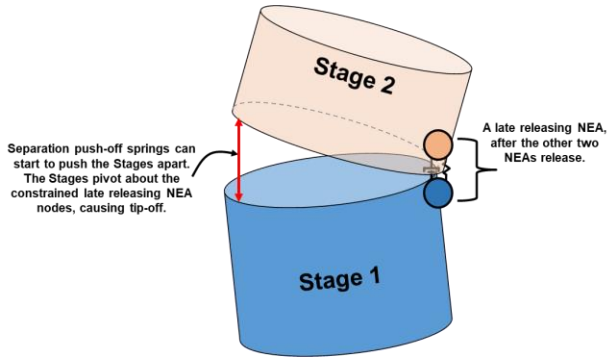

Figure 13. NEA Simultaneity Variance

Although the LSSN was determined to provide the best orbital accuracy, a series of additional figures of merit were examined to compare its overall capability with the clamp band system. Items such as mass, impact of aeroheating environments, expected induced shock environments, heritage, and integration with existing systems were assessed. Ultimately, the LSSN was selected as the baseline stage separation mechanism, primarily due to its low contribution to tipoff rates, low protuberance from the vehicle, and low mass. A rigorous test scheme is planned for both systems. The clamp band system will be held in reserve in the event that target parameters cannot be met by the LSSN system. The baseline LSSN is shown in Figure 14, with aero fairing removed for illustration.

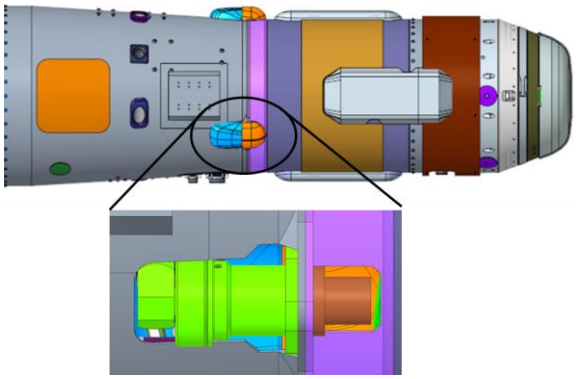

Figure 14. Baseline LSSN Stage Separation Mechanism

7. THERMODYNAMICS

All hardware components aboard the MAV have specific temperature ranges in which they are designed to operate. Some are largely unaffected by temperature, whereas others must be kept within carefully controlled temperature ranges. While not in active use, all components will be kept at their non-operational Allowable Flight Temperature (AFT). The non-operational configuration is mostly employed while the MAV is stowed within the SRL and MLP, including launch from Earth through Mars surface operations. During this time, the MAV will be mostly dormant. Prior to the actual flight mission, all components will be brought from non-operational AFT to operational AFT. While stowed aboard the MLP, the MAV will be contained within a thermal enclosure, or "igloo". This will maintain a consistent external temperature and will provide an additional layer for protection against extreme mission environments prior to the flight mission. The igloo will only be exposed to the Martian environment just prior to VECTOR ejection. The MAV-SRL igloo configuration is conceptually shown in Figure 15.

Although the integrated vehicle itself will be held at non-operational AFTs during these times, several individual components, such as the flight computer and TVC, will be brought up to operational AFTs during cruise to Mars and surface operations. This will be done to perform any calibrations and safety checks. Following these checks, said components will return to their non-operational state.

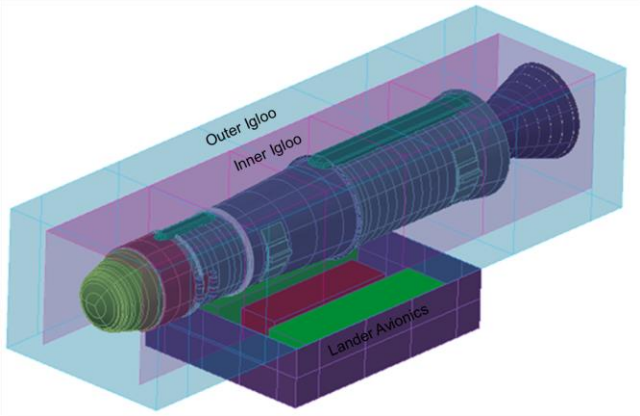

Figure 15. SRL with MAV Stowed Within Igloo

The final warmup from non-operational AFTs to operational

AFTs will begin approximately two weeks prior to the flight mission. Some components, such as SRMs, are extremely sensitive to large pressure gradients. Changes in temperature must be introduced slowly to reduce differences in thermal expansion. Once all components are at adequate operational AFT, the top of the MLP will open in preparation for ejection. During ascent, there will be no active heating on the majority of the vehicle, as the flight mission is short enough where passive temperature losses will not be an issue. The exception to this is for beacon operation. The beacon must operate for up to 25 days following orbital insertion of the OS. During this time, it must be actively heated. Beacon functionality is described more in Section 8.

In order to maintain adequate AFTs during the MAV mission, a Thermal Control System (TCS) was designed. The TCS combines active and passive hardware. The TCS will support non-operational temperatures during dormant phases of the MAV mission and raise temperatures in preparation for active phases. Most components aboard the MAV have their own individual AFT ranges. As it would be impractical to heat each component individually, the MAV was divided into 15 individual heater zones, based upon hardware needs and grouping. The avionics, for example, being mostly electronics-based, must all be kept at relatively similar temperatures. In this case, if the flight computer must be brought up to operational AFTs, all hardware within the same thermal zone would be brought up to the same temperature. The 15 integrated vehicle thermal control zones of the TCS are shown in Figure 16.

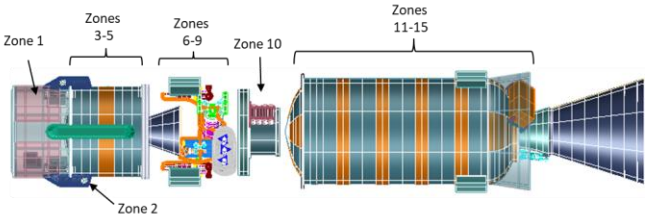

Figure 16. Integrated Vehicle Thermal Control Zones

The active portion of the TCS features Platinum Resistance Thermometers (PRTs), mostly controlled and powered directly by the SRL computer. Once the MAV has separated from the lander, the only remaining active TCS components will be in support of the aforementioned beacon. Passive thermal protection is included in the design in the form of insulation and thermal isolators. In addition to helping to trap heat within each control zone, this Thermal Protection System (TPS) prevents high external temperatures during ascent from induced environments such as aeroheating and plume radiation.

For the majority of the MAV mission, the vehicle exterior will be maintained at -62.5°C by the SRL igloo. Most internal components will be kept at a non-operational AFT of -40°C and an operational AFT of -20°C. As mentioned in Section 5, the RCS features a hydrazine-based monopropellant. This introduces a unique thermal design challenge, as hydrazine freezes at 2°C. This is substantially higher than most MAV hardware's operational AFT. For this case, a special set of heaters with higher performance was selected, at the expense of more electrical power. The RCS requires a temperature of at least 14°C in all individual zones to allow optimal RCS operation with a healthy temperature margin. RCS thermal zones are shown in Figure 17. Note that these zones have a different number convention from the integrated thermal model.

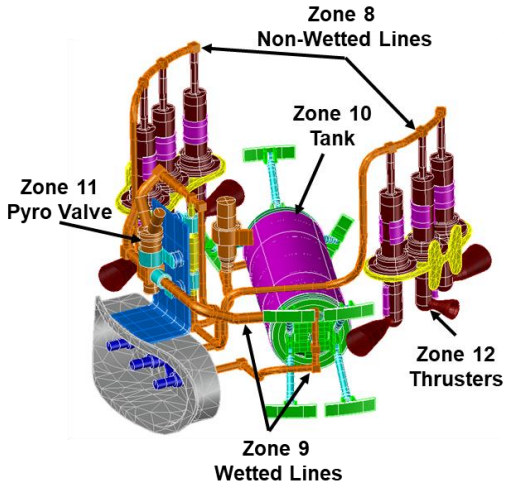

Figure 17. RCS Thermal Control Zones

Sizing of MAV thermal components is largely affected by Martian natural environments. Although the Jezero Crater launch site is fairly close to the Martian equator, its average temperatures are extremely cold by typical launch vehicle design standards. As shown in Figure 18, the average Martian diurnal cycle could result in the MAV experiencing external temperatures as low as -130°C during its mission, even if it were to fly on the Martian Summer solstice.

For the thermal design and analysis, MAV ascent was considered for both Summer cases (Solar longitude, L_s = 90°) and the beginning of Martian Autumn (Solar longitude, L_s = 173°). A Martian winter launch was not considered, as such extreme temperatures would introduce unnecessary complexities to the design. The MAV will only be exposed to the extreme Martian temperatures just prior to and during ascent. As mentioned previously, this will only be on the order of minutes, and will therefore not require an active TCS outside of beacon operation.

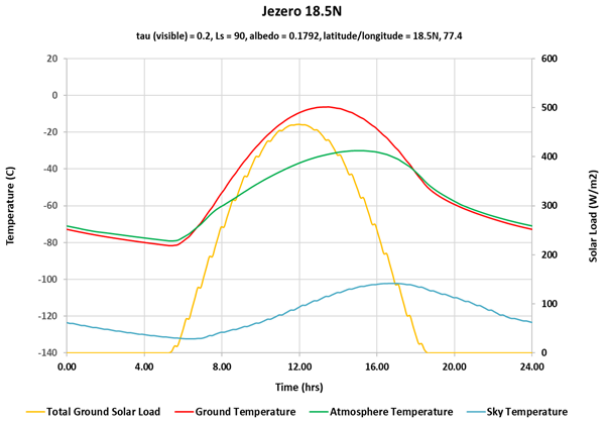

Figure 18. Average Martian Temperatures, L_s=90°

The passive TPS design was developed following an analysis of an integrated vehicle ascent heating profile. This took into consideration all sources of heat that may affect the MAV, including external aeroheating, plume radiation, SRM nozzle and case thermal soak back, avionics waste heat, and solar energy. The thermal distribution across the vehicle exterior during first stage flight is shown in Figure 19. Peak ascent heating temperatures were observed at approximately 80s into flight. Some protuberances, notably the spin motor housings and cabling pass throughs (circled in red) encountered temperatures in excess of 150°C, mostly due to ascent aeroheating.

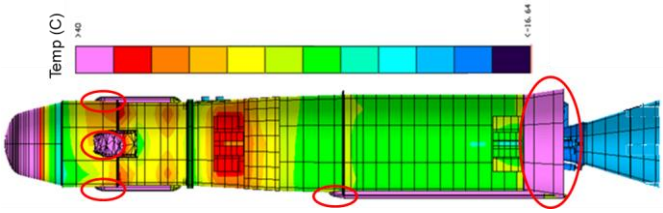

Figure 19. Peak External Temperatures

The largest temperatures were observed at a stagnation point at the tip of the MPA during ascent. This stagnation point experienced temperatures of in excess of 300°C. The temperature distribution across the MPA is shown in more detail in Figure 20.

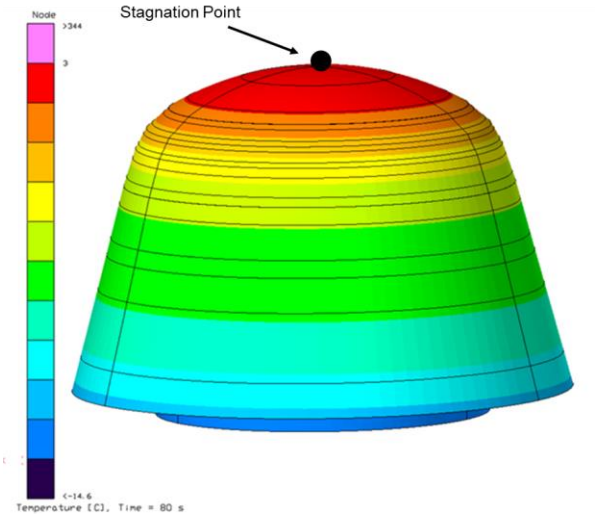

Figure 20. MPA Peak External Temperatures

Figures 19 and 20 show significantly higher temperatures than the assumed upper hardware limits of the internal MAV components. The TPS was sized accordingly to prevent the AFT operational temperatures from being exceeded. The peak temperatures circled in Figure 19 represent areas that may need additional TPS design work in the future.

8. AVIONICS

The MAV avionics system is primarily responsible for three functions: command and data handling, power distribution, and communication. Because only the first stage of the MAV is guided, the majority of avionics components are located on the first stage. This constitutes the primary avionics shelf and consists of an Inertial Measurement Unit (IMU), transmitter, Power Distribution Board (PDB), RCS controller, pyrotechnical controller, Mission Unique Card (MUC), flight computer, and internal batteries. Where applicable, these components will be connected to the MLP via umbilical interface for transfer of power and data. Additional cabling will run throughout the vehicle, providing an internal interface to various sensors and mechanisms. The primary avionics shelf is located in the vehicle interstage, between SRM1 and RCS. The hardware layout of the primary avionics is shown in Figure 21, inverted for clarity.

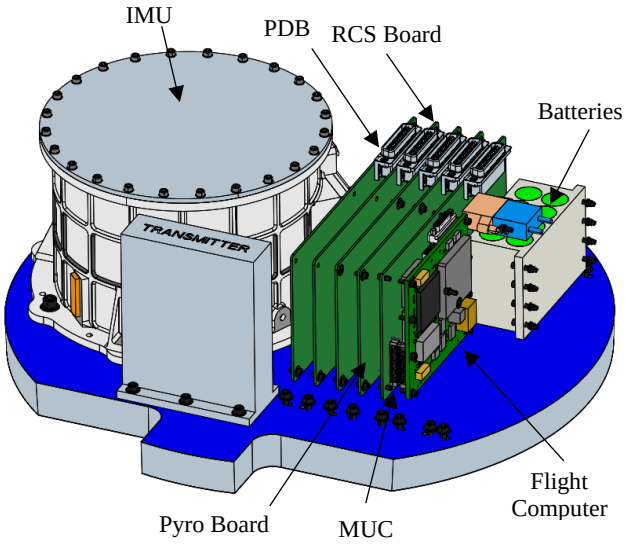

Figure 21. Primary Avionics Hardware Layout

Following stage separation, the MAV will enter an unguided, spin-stabilized phase of flight. During this phase, the remaining avionics components are limited to a timing circuit, beacon, batteries, heaters, and an antenna. These compose the secondary avionics. Although positioned on the second stage, the antenna will be used by the transmitter during first stage flight and the beacon following stage separation. A coaxial cable connector will span the separation plane, connecting the transmitter on the first stage to the antenna on the second stage. The hardware layout of the secondary avionics is shown in Figure 22, with cover removed on beacon boards and batteries for clarity. The antenna is absent from this image as it is bonded to the external skin of the MAV. Note that a series of thermal isolation bolts are present. These are vital to the long duration operation of the beacon.

Primary command and data handling is managed by the flight computer, IMU, and various controller boards. Although the vehicle will have a set of operational flight instrumentation, they are considered hardware for their respective disciplines. Interface with the flight computer is performed via cabling. The flight computer is the “brain” of the vehicle and is responsible for execution of all algorithms and commanding of all activities of the vehicle. For this application, a Coyote flight computer was selected. This computer was developed by NASA JPL for use on small scale vehicles with srict mass and power restrictions, while having a high tolerance to radiation. The flight computer interfaces with all other components via the Mission Unique Card (MUC).

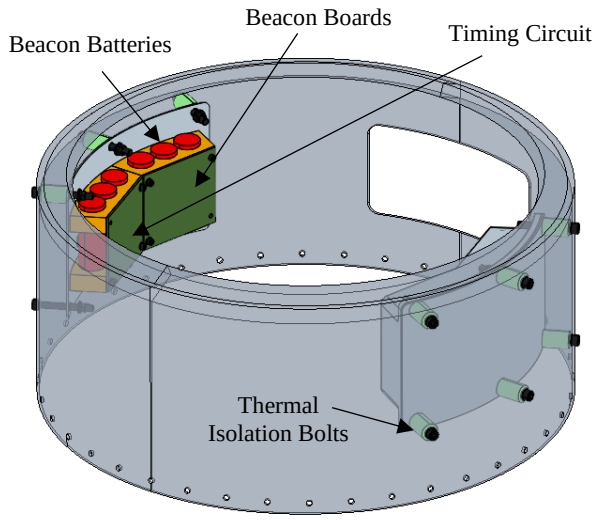

Figure 22. Avionics Hardware Layout

The aforementioned IMU is vital for determining the vehicle attitude during flight. Although most instrumentation onboard is owned by other elements, the IMU is considered an avionics piece of hardware. For this application, a Honeywell Miniature Inertial Measurement Unit (MIMU), or similar, was selected. Most IMUs for vehicles of this size are significantly smaller due to their typical operation in Earth-based sounding rockets. These rockets experience significantly more benign environmental conditions. Although significantly larger than the other avionics components, this IMU has a lot of heritage in both Mars and deep space missions.

Custom controller boards are planned for operating the RCS and pyrotechnics. Although the flight computer will initially determine when the RCS and pyrotechnics will need to fire and in what orientation, the respective controller boards will determine how the RCS and pyrotechnics will actually operate. It should be noted that although the flight computer also commands the TVC, the TVC controller board itself is located on the aft end of the vehicle directly next to the TVC actuators themselves. While stowed aboard the SRL S/C, the MAV avionics will interface with the SRL S/C avionics through a series of umbilical connections. These will provide active power for the MAV TCS and batteries, as well as aid in the reporting of telemetry prior to the MAV ascent mission. Items that will need calibration, such as IMU gyrocompassing, will also be confirmed via lander umbilicals. Secondary command and data handling following stage separation is extremely limited. At this point, a simple timer circuit is planned. This will execute commands in a time-based sequence without any feedback. In the future, a FPGA or microcontroller may be used for additional second stage computational processing.

For primary avionics power and power distribution, onboard batteries and a custom PDB was developed. The power source selected for the SRC was a package of eight LG MJ1 18650 3500mAh 10A batteries. These batteries are expected to have reliable long-term performance during the extended MAV stowed phase and would be recharged by MLP solar panels following any passive discharge. The batteries themselves would only provide power to avionics systems and mechanisms during the MAV ascent mission; while stowed aboard the MLP, MLP power systems will provide direct power as needed via umbilical interfaces. For secondary avionics, a package of twelve of the same batteries were selected. Although flight operations of the second stage MAV has a relatively low power demand, the beacon must operate for up to 25 days, requiring significantly more power for heaters.

The transmission of flight telemetry will be performed via a transmitter on the first stage. This will broadcast telemetry for flight trajectory recreation and critical events coverage back to Earth via the Mars Relay Network (MRN). Due to the tremendous distance between Earth and Mars, is expected that ground operators will not begin receiving this telemetry until after the actual MAV ascent has concluded. For the SRC, an L3 Harris transmitter, or similar, was assumed with a basic wraparound antenna on the second stage. Further studies have since developed this antenna following the SRC. Within the current concept of operations, a navigational beacon will broadcast a simple signal via the antenna following stage separation. This will be the only piece of information broadcasted from the MAV following stage separation. The ERO will receive this signal and use it to determine the approximate location of the MAV spent second stage. From there it will use optics to visually sight the second stage, and then extrapolate the position of the OS in relation to the MAV. The beacon is required to remain operational for up to 25 days, presenting an interesting design challenge. Although the beacon itself does not use a significant amount of power, it must remain at an operational temperature of at least -20°C, meaning a non-trivial amount of mass must be included for both heaters and heater batteries. The beacon will operate in two modes, commanded by the second stage timing circuit. The first mode, known as “siren-mode” will activate immediately following stage separation, and broadcast a signal in rapid succession. The second mode, known as “lighthouse-mode” will activate following OS ejection, and will broadcast a signal at a lower frequency. This will allow for Earth operators to know when different aspects of the mission have completed, without the need for a transmitter on the second stage.

Flight Software & Mission/Fault Management

MAV Flight Software (FSW) is responsible for overseeing the execution of all nominal and off-nominal mission operations through its command and data handling capability. FSW integrates control algorithms and mission management functional algorithms within its framework. FSW programming will be executed by the flight computer, where it will interface with external entities and internal subsystems. FSW development follows an incremental approach with the capability to perform ascent operations at any point during the lifecycle. Source code is configuration managed and regularly updated as the vehicle design lifecycle progresses. The operating system environment for FSW is Real-Time Executive for Multiprocessor Systems (RTEMS). It will use

a Goddard Space Flight Center (GSFC)-developed, open-source core Flight System (cFS) architectural framework. cFS will also be used in the simulation of hardware components for functional and integration testing in a Software Integration Lab (SIL). Initial algorithms to satisfy nominal and off-nominal mission requirements were developed utilizing Model-Based Systems Engineering (MBSE). Algorithms are based on engineering drawings, Interface Control Drawings (ICDs), and subsystem Concepts of Operation (CONOPS). The algorithms are converted into tables that can be run directly with standard cFS applications. Traditional text-based requirements will be derived in part from the developed algorithms.

9. AEROSCIENCES & ENVIRONMENTS

Despite Mars having an atmospheric density of less than 1% of that of Earth, it is still dense enough for the vehicle to create induced aeroscience-based environments. Understanding of these environments is necessary to ensure the survival of all hardware components aboard the vehicle. Analyses were performed to generate environments related to aerodynamics, acoustics, and shock/vibration.

Aerodynamics

Aerodynamic analysis is crucial for the understanding of how the vehicle will respond to the Martian atmosphere during ascent. Shape analysis of the vehicle began with an assessment of the vehicle OML. Elements such as protuberances and sharp corners can create large aerodynamic surface pressures and shockwaves at various points in the trajectory. Earlier MAV cycles featured low fidelity empirical methods for initial aerodynamic modeling. The SRC design, however, required more comprehensive CFD analysis, based upon the vehicle design itself. A series of CFD-based analyses were performed using the FUN3D suite of tools to generate an aerodynamic database of pressure coefficients across the vehicle. These were used as aerodynamic line loads in the integrated loads model described in Section 6, and as aerodynamic disturbance torques in the GNC design described in Section 10. The CFD analysis considered a Mach range from subsonic through hypersonic velocities at various angles of attack. Sensitivity to protuberances, plume effects, and RCS interactions were also investigated. Figure 23 shows an example pressure distribution across the vehicle surface.

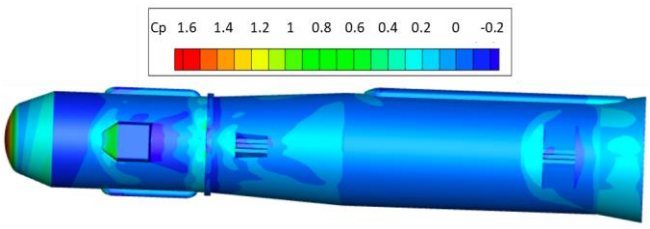

Figure 23. Sample Pressure Distribution

A CFD powered flight analysis was also performed. This was done to quantify differences in aerodynamic coefficients due to motor plume and to determine the sensitivity of plume flow to gas chemistry modeling. Noticeable engine-on effects were observed at transonic conditions. These were negligible at hypersonic velocities. The gas chemistry reaction models were found to not affect the motor plume significantly. Differences in velocity between powered-on and powered-off flight at maximum dynamic pressure are shown in Figure 24.

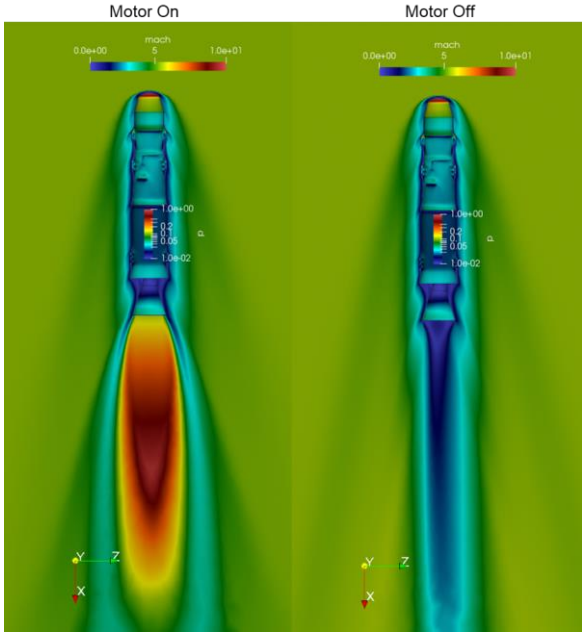

Figure 24. Effects of SRM1 Plume

Ultimately, the CFD analysis predicted the vehicle to be statically unstable across most of its ascent, with the largest instability observed at large angles of attack near transonic flight regimes. It should be noted that aerodynamic instability does not necessarily mean that the vehicle cannot be controlled. A robust control scheme, as defined in Section 10, can mitigate the instability. Figure 25 displays the aerodynamic stability at two points in the vehicle. Pitching moment, Cmα, is shown to be negative at the vehicle nose at all Mach numbers examined. Pitching moment is only marginally positive aft of the nose.

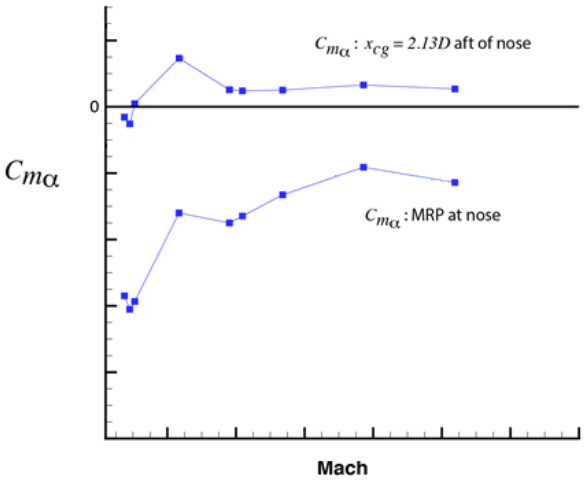

Figure 25. Aerodynamic Stability

Buffet Environments

An initial assessment of the MAV SRC OML raised concerns about transonic buffet environments due to several factors such as the blunt nose, large protuberances, and wake on the engine nozzles. To support an assessment of the buffet impact, a preliminary Buffet Forcing Function (BFF) database was developed. As with aerodynamic line loads, these unsteady aerodynamic buffet loads were included in the integrated loads model described in Section 6. This MAV BFF database was a preliminary release, using data from a recent NASA Ames Research Center (ARC) Unitary Plan Wind Tunnel (UPWT) test of a 2.5% scale Space Launch System (SLS) Block 1 Cargo rigid buffet model, shown in Figure 26.

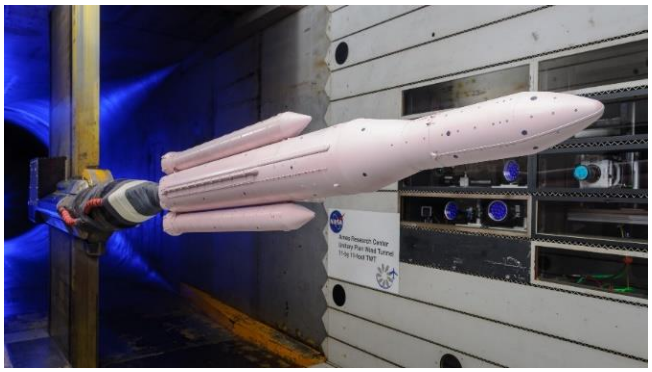

Figure 26. Wind Tunnel Model Scaled for MAV

Regions of the SLS model were mapped to similar regions of the MAV, shown in Figure 27. Once the model was scaled, integration boundaries were defined for each pressure transducer. Fluctuating pressures were integrated over their respective surface panels. Several tunnel tones were attenuated to reduce impact of tunnel noise. Finally, the data were geometrically scaled to the full-scale MAV using rigid buffet scaling laws. Trajectory scaling will be updated as more recent MAV trajectories are released.

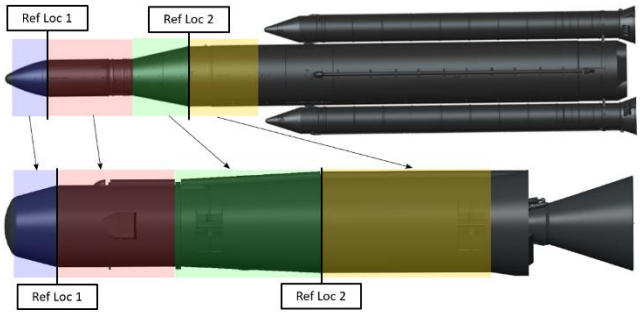

Figure 27. Buffet Model Scaling Regions

Using MAV trajectories, accelerating flight CFD simulations were run to generate predicted sectional and point loads on the vehicle. These CFD simulations captured items such as protuberance and blunt nose impacts while accounting for Reynolds number effects. The SRC BFF database was intended to serve as a preliminary estimate on the magnitude and characteristics of buffet loads on the MAV. A more detailed database will be developed in future analysis cycles based entirely on the MAV OML rather than scaled wind tunnel data. Future wind tunnel testing of MAV models will further anchor these predictions.

Vibration, Internal Acoustic, and Shock Environments

Both random and sine vibration environments were developed for the SRC configuration. Random vibration environments were derived from the vibratory energy generated by acoustic loading of the external and internal vehicle surfaces and from structural transmission of energy from SRMs and mechanisms. Sine vibration environments account for low frequency transient environments induced by the vehicle as a result of the various vehicle load events throughout the mission. Low frequency vehicle transients are specified as acceleration time histories and shock spectra. Sine vibration environments are only used as a design aid for secondary structures in mounting of items such as avionics hardware. Although Mars launch is the primary consideration for MAV performance, Earth launch and Mars EDL vibration environments were also developed. For this analysis, the vehicle was divided into six individual zones, shown in Figure 28. These zones were also used for acoustic analyses. Maximum Predicted Environments (MPEs) were defined for components in each of these locations, incorporating location, design, and mass details of each component. Internal acoustics were defined in the form of Sound Pressure Level (SPL) MPEs for Earth launch and Mars ascent. Mars ascent acoustics were of most interest in zones S1 through S4, due to the various open compartments within them.

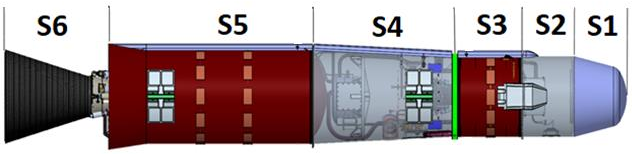

Figure 28. Acoustic & Vibration Zones

An analysis was performed to determine peak acceleration during induced shock events. These events were defined as VECTOR ejection, stage separation, and MPA fairing separation. The shock levels accounted for attenuation from structural joints. MPA fairing shock, although induced by pyrotechnics, was not found to be a significant source of peak acceleration to any hardware. The LSSNs described in Section 6 provided a similar response. The VECTOR ejection shock environments are of potential concern to RCS hardware, however, and are being examined in more detail.

External Acoustics

As a launch vehicle accelerates during ascent, the fluctuating pressures on the surface of the vehicle vary in proportion to free stream dynamic pressure. These pressures are mostly associated with boundary layer turbulence, flow separation, flow reattachment, and shock waves. Ascent aeroacoustics environments capture the noise generated by these unsteady flow features. MPEs in local areas depend on flight orientation, vehicle mechanical design, and Mach number. Traditional time accurate responses of these flow features can be difficult to capture with mathematical methods. High-

frequency pressure transducers in wind tunnel testing is often found to be more effective.

Preliminary aeroacoustics assessments were estimated in a similar manner as described with buffet environments: scaling of SLS wind tunnel data from regions of like geometry to a MAV design trajectory. Wind tunnel data for aeroacoustic scaling was only available in transonic and supersonic flow regimes. The maximum expected dynamic pressure for MAV, however, is expected to be encountered during hypersonic velocities. In order to adequately apply the SLS wind tunnel data, an aeroacoustic design trajectory was derived by scaling the GNC 3DOF trajectory described in Section 10. This was scaled so that the dynamic pressure at the observed SLS wind tunnel supersonic Mach limit was equal to that of the MAV expected maximum dynamic pressure. Although this does result in a somewhat more conservative estimate of environments at transonic velocities, it adequately captures expected MAV aeroacoustic behavior. Above approximately Mach 1.5, all dominant flow features are expected to stabilize, meaning that from an unsteady flow perspective, environments at higher Mach numbers would be similar. Ascent aeroacoustic environments were developed as MPE SPLs across all Mach numbers tested with a variety angles of attack. Acoustic zones were grouped similarly to the internal acoustic zones displayed in Figure 28. The loads from these SPLs were included in the integrated loads model described in Section 6.

Aside from ascent aeroacoustics, liftoff and plume-induced acoustic environments were also calculated. Liftoff acoustics account for noise generated from SRM exhaust interacting with surrounding atmosphere and launch structures. Plume-induced acoustics account for noise from SRM exhaust interacting with surrounding aerodynamic flow. The MAV SRC design for these iterated on previous configurations to improve overall mission readiness and capability. As with other acoustic environments, liftoff and plume-induced acoustics leveraged a semi-empirical model to scale legacy data captured from earlier launch vehicles. This data included motor plumes of similar thrust class rather than large scale vehicles such as SLS. Scaling was done in both amplitude and frequency, through intensity and Strouhal number, respectively. Scaling of data from Earth to Mars atmospheric conditions was achieved with a log-ratio of the characteristic impedance of each atmosphere, dropping the expected sound level by an appropriate magnitude at all vehicle locations. Propagation throughout the vehicle body was estimated using the Prediction of Acoustic Vehicle Environments (PAVE) tool, relative to a source at the Nozzle Exit Plane (NEP). Propagation through the Martian atmosphere was predicted using an atmospheric attenuation model coupled with intensity scaling relative to the NEP. The high acoustic impedance of the Martian atmosphere was found to result in a weaker acoustic source strength than Earth environments, with acoustic disturbances that are expected to attenuate faster.

10. GUIDANCE, NAVIGATION, & CONTROL

Mission Analysis, Guidance, and Navigation

The ultimate goal of the MAV mission is to deliver the sample tube payload from the Mars surface to orbit. Although the vehicle design presented previously details the individual systems and components, the ultimate success of the integrated vehicle is reflected in its final orbit state. All individual designs contribute to this performance and must be taken into account when designing and optimizing the orbit. For this design cycle, the MAV trajectory was nominally designed to target an orbit of 380km. Other significant trajectory parameters included inclination angle, Semi-Major Axis (SMA), eccentricity, and Right Ascension of the Ascending Node (RAAN).

To achieve this target orbit, design of the aforementioned attitude control systems was considered with SRM thrust parameters and vehicle mass properties. Due to the unguided second stage, it is absolutely necessary that a robust Guidance, Navigation, and Control (GNC) scheme be employed to ensure the vehicle is in the correct state following stage separation. The RCS was designed for roll control during first stage burn and full control about all axes during coast. The TVC was designed for pitch and yaw control during first stage burn. Initial mission analysis began with preliminary estimates of motor performance. With updated vehicle mass allocations from the previous design cycle, early sizing of SRMs gave an approximation on vehicle size, thrust profile, and mass properties. These allowed for the development of a 3 Degrees-of-Freedom (3DOF) trajectory, using only translational movement of a point mass and neglecting things such as attitude and second stage spin rate. Following initial 3DOF development, an iterative process allowed for fine tuning of SRMs based upon required thrust. Once 3DOF trajectories were complete, a Mass Estimate List (MEL) was developed in accordance with all other systems to create a detailed record of all hardware items on the vehicle. This, combined with environments, such aerodynamics shown in Section 9, was used to create a nominal 6 Degrees of Freedom (6DOF) model of the vehicle ascent. The high-fidelity 6DOF simulation took into consideration vehicle attitude, induced and natural environments, and mission-specific activities such as a second stage spin stabilization. The 6DOF model ultimately determined the vehicle attitude needed to achieve the desired orbit, allowing for development of guidance algorithms and controllability through RCS and TVC.

Figure 29 describes the 6DOF flight plan. Following VECTOR ejection from the MLP, the SRM1 will ignite and the vehicle will be under closed loop guidance for the duration of SRM1 burn. After burnout, the vehicle will enter an attitude hold phase during coast as it approaches apoapsis. Closed loop guidance will continue in this segment, maintaining the flight vector. During coast, the flight computer will calculate the most optimized time to initiate stage separation and ignite SRM2 as part of an energy

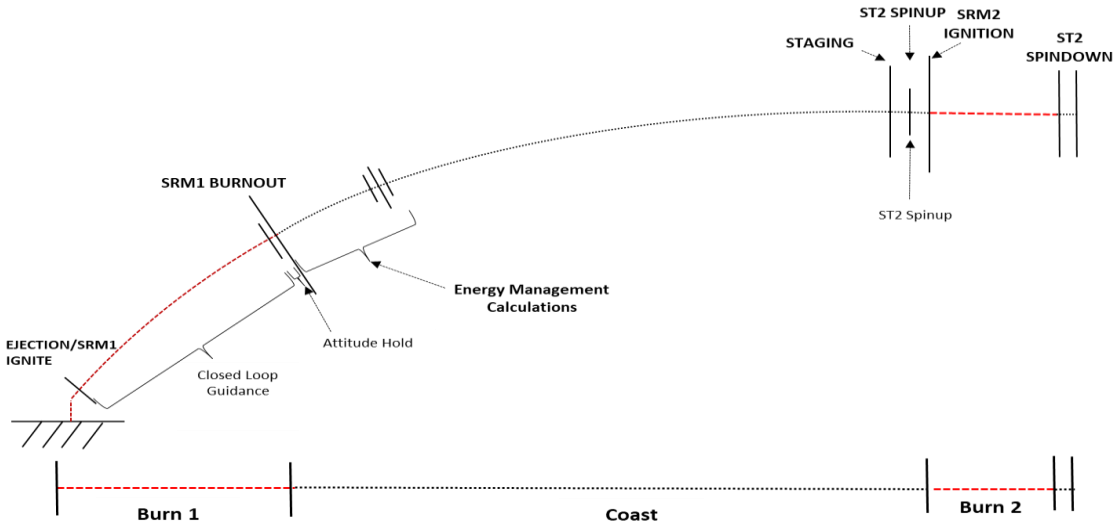

Figure 29. Vehicle Flight Plan

management maneuver. Typically, an impulsive circularization burn is most efficient when performed at apoapsis. In this case, however, as the vehicle features solid propellant, it cannot actively throttle or shutdown. The energy management maneuver performs SRM2 burn prior to apoapsis, expending excess energy by performing an apse line shift. As the vehicle approaches the end of coast, it will orient away from the flight vector for MPA fairing separation, before reorienting for stage separation. Nominal separation would not include tip-off rates, however, these are included in dispersed analyses. Immediately following stage separation, the second stage spin-up occurs, followed by SRM2 ignition. SRM2 burn is relatively short and only exists to raise the periapsis. During this phase, the vehicle will be entirely unguided. Spin down occurs well after initial SRM2 burnout to allow for any shutdown transient thrust to be released with no negative effect on the trajectory. Once the second stage has completed spin down, the vehicle will be at the desired orbit and attitude for OS release.

The nominal trajectory is useful for determining target orbit and parameters. The actual vehicle performance, however, will be largely affected by variations in the manufacturing process and uncertainties in the mission environment. The payload, for example, is expected to be 16kg. The actual composition and density of the Martian samples will actually be unknown. This will result in an unknown payload mass distribution. For this reason, the guidance and control algorithms must be robust enough to support any reasonable variations.

The trajectory analysis found that all mission design constraints were met with nominal input parameters. A series of dispersed analyses were conducted to determine vehicle response to the aforementioned variations and uncertainties. Three sigma dispersions were included on over 80 individual input parameters, such as moments of inertia, aerodynamic coefficients, and thrust misalignments. Combinations of these dispersions were introduced through a Monte Carlo analysis. This found that, as expected, there was a significant amount of scatter on the orbit apoapsis and periapsis, compared to previous guided second stage options. Despite this, only one case out of 2000 was observed to fall below the 300km periapsis constraint. Three cases were found to exceed the SMA constraint. Figures 30 and 31 summarize the dispersed results in relation to altitude and RAAN/inclination.

As mentioned in Section 6, a trade study was performed to determine the most effective stage separation mechanism for this application. Although the trade mostly involved the structural capabilities of the three trade candidates, the GNC performance was also a key driver. GN&C analysis was focused on understanding, modeling, assessing, and identifying design improvements in two distinct, but coupled, areas related to MAV separation. The first was near-field separation performance and clearance, ensuring the two stages would successfully separate without recontact between the small clearances of the interstage hardware and the nested SRM2 nozzle. The second was final stage 2 orbital accuracy,

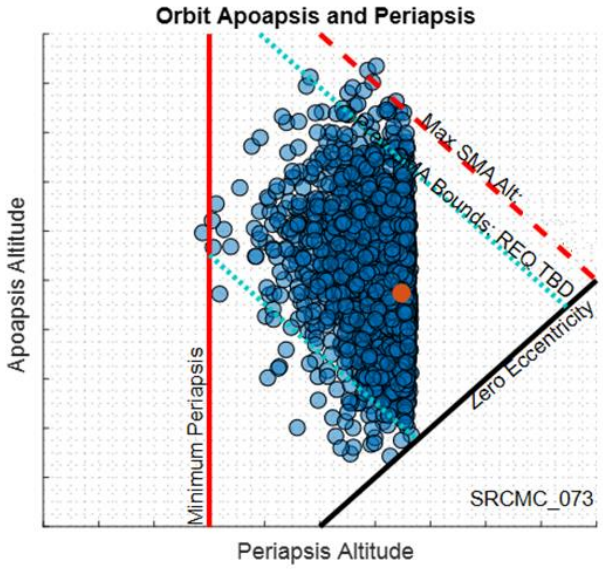

Figure 30. Orbit Altitude Variation

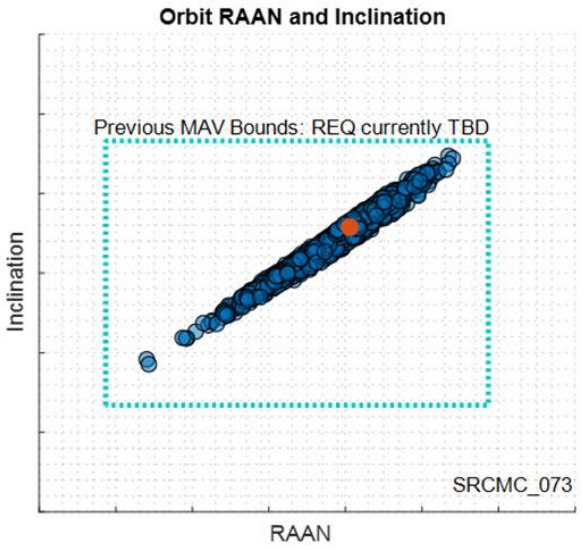

Figure 31. Orbit Inclination and RAAN Dispersions

assessing how separation disturbances propagate through the stage 2 trajectory and impact the final orbital accuracy of the OS. Figure 32 depicts the stage separation clearance necessary to avoid recontact. Separation dynamics and clearance analysis used a multibody 6DOF simulation tool with CAD models to calculate clearances during the separation event.

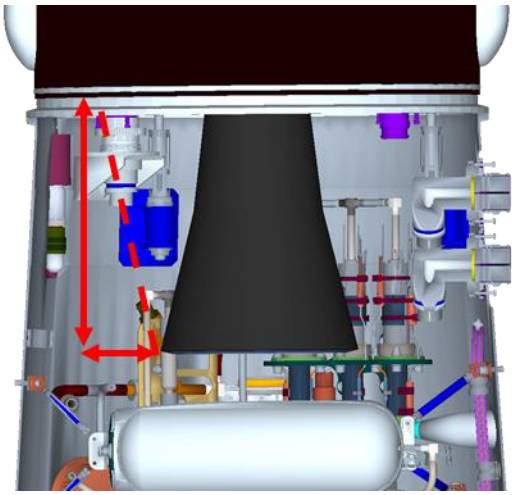

Figure 32. Stage Separation Clearance

Monte Carlo clearance analysis used similar dispersions as the GNC ascent trajectory 6DOF simulations, with more emphasis on items such as mechanism spring force and stroke profiles rather than time histories. Individual Monte Carlo analyses were run with each of the aforementioned three candidate separation mechanisms (See Section 6). It was found that although initiating the second stage spin-up as early as possible significantly helped with orbital insertion accuracy, the stage separation clearance likelihood decreased, making recontact more probable. Ultimately, pointing error could still be minimized at the end of stage 2 spin-up while ensuring near-field separation was met in each of the candidate cases. Between the NEAs, clamp-band, and LSSNs, preliminary assessments showed more favorable orbital performance with the LSSNs compared to the other two options. This was included as a figure of merit in the overarching trade study. An example comparison of stage separation orbital results is shown in Figure 33.

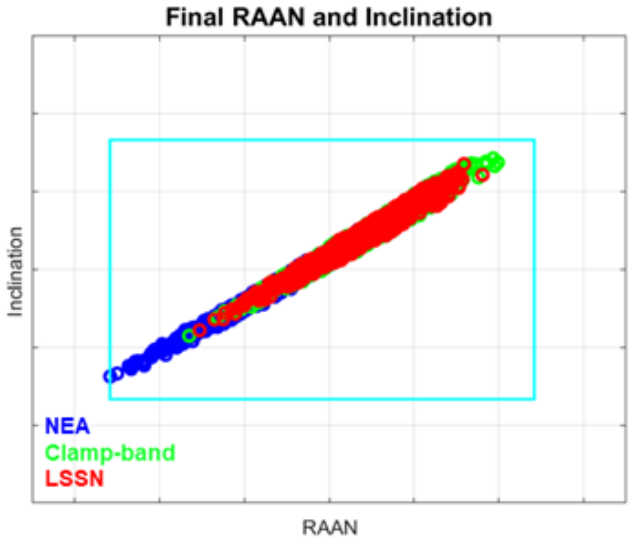

Figure 33. Stage Separation Mechanism Orbital Results

Stability & Control

Although the vehicle guidance algorithms within the flight software are designed to keep the vehicle aligned with its target trajectory, it is up to the various controller designs to determine the necessary output to do so. This is achieved through actuation of the attitude control devices. The flight computer determines where the vehicle needs to be and how it must be oriented, while the RCS and TVC controller boards determines how each of those systems must react. They must also be robust enough to overcome any disturbance torques during flight. For the TVC, this translates to pitch and yaw commands during SRM1 burn. For the RCS, this translates to a thrust level about the roll axis during SRM1 burn and about all axes during coast. Development of the control logic behind both systems was necessary for a successful GNC system.

The TVC system control scheme was designed using a second order transfer function. This integrated dynamics from the SSSL TVC system detailed in Section 5. The controller itself featured Proportional-Integral-Derivative (PID) logic. This used navigational measurements from the IMU and guidance states from the flight computer as input. PID gains were pole-placed to enable adequate control margins throughout ascent. The TVC control scheme is shown in Figure 34. Slosh and flexible body dynamics were not considered for this design. Note that this only applies to the first stage as no TVC exists on SRM2.

Industry standard stability margins were used as a measure of effectiveness of the TVC controller. Gain margin measures absolute stability and the degree that a system will react to a given disturbance. A system is considered gain stable if it has

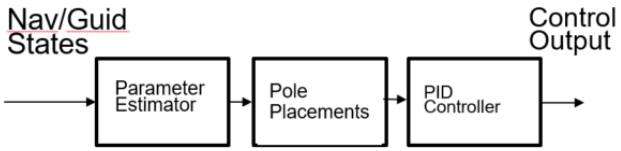

Figure 34. TVC Control Scheme

a gain margin of at least 6 dB. Phase margin measures relative stability and how a system will react during a damped response to an input. A system is considered phase stable if it has a phase margin of at least 30°. Together, these margins measure the vehicle's resistance to becoming unstable. For the MAV SRC, TVC stability margins were determined throughout first stage flight. The design demonstrated adequate stability margins for both gain and phase.

The RCS system was represented by an instantaneous torque upon the vehicle. This was produced from thrust from the RCS nozzles via propellant look-up tables. The control system was designed as a phase plane type controller, employing torques based on pointing error dynamics. Roll, pitch, and yaw all had separate phase planes. Thruster firings were determined via a nozzle-select corresponding to Euler angle torque commands. Startup and shutdown transients were not considered for the RCS nozzles. The overall RCS architecture was designed to maintain acceptable control authority with acceptable stability and propellant margins. As described in Section 4, the updated SRC vehicle design features the RCS frame unaligned with the body frame. Guidance commands must account for this rotation. The RCS nozzles themselves are also located significantly closer to the vehicle CG, resulting in a considerably smaller moment arm during coast and a decrease in overall control authority. Overall RCS controllability criteria were determined through comparison of expected control torque with that of external disturbances and gyroscopic effects [7], shown in Equation 1. This measures how well the RCS is sized and placed compared to expected environments and dynamics throughout time. It is desirable to have a control ratio of 2 or higher throughout RCS operation.

$$Controllability = \frac{T_{Control}}{T_{Gyro} + T_{Dist}} \geq 2 \quad (1)$$

RCS controllability and stability responses were derived for two phases of flight including first stage burn and coast. Controllability is only provided in all axes during coast. As with TVC, at least 6dB gain margin and 30° phase margin were used to determine stability. The controllability study featured Monte Carlo analysis for SRM1 through stage separation. Throughout the two flight phases examined, roll control remained well above the criteria established in Equation 1. For pitch and yaw, however, a control ratio of less than 2 was observed for a short transient at the end of SRM1 burn due to aerodynamic torques. These results are summarized in Figure 35.

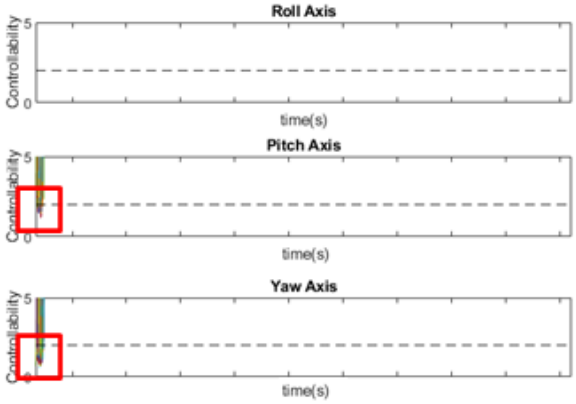

Figure 35. RCS Controllability

A closer look at these points regarding stability revealed phase margin violations for pitch and yaw. Once again, roll had no violations. This is displayed in the Nichols plots in Figure 36.

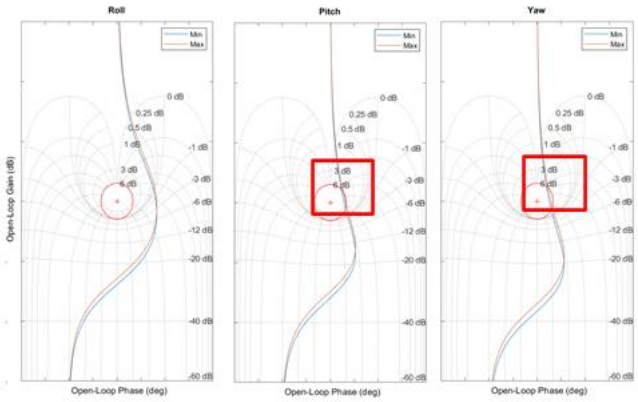

Figure 36. RCS Stability

Both the low control authority and instability observed were a direct result of the significant decrease in RCS moment arm. Although there was limited capability to alter the moment arm from a GNC perspective, the RCS controller parameters were able to be tuned to improve stability. Investigation revealed that the reduction in moment arm largely decreased the vehicle's angular acceleration response to RCS torques. This in turn acted to provide less static gain, shifting the Nichols response down. By retuning the deadband and rate limit, the parameters for the phase plane were adjusted, resulting in considerably improved stability margins in pitch and yaw axes. The updated pitch and yaw stability is shown in Figure 37. Although the update to the phase plane parameters showed acceptable stability margins, the controllability ratio about pitch and yaw axes remains sub-optimal towards the end of SRM1 burn. This can be addressed in future design cycles by either increasing the moment arm or reducing aerodynamic torques. The moment arm can be increased by either shifting the axial location of the vehicle CG or shifting the axial location of RCS thruster nozzles. The aerodynamic torques can be reduced by changing the SRM1 burn time to achieve burnout outside of the sensible atmosphere.

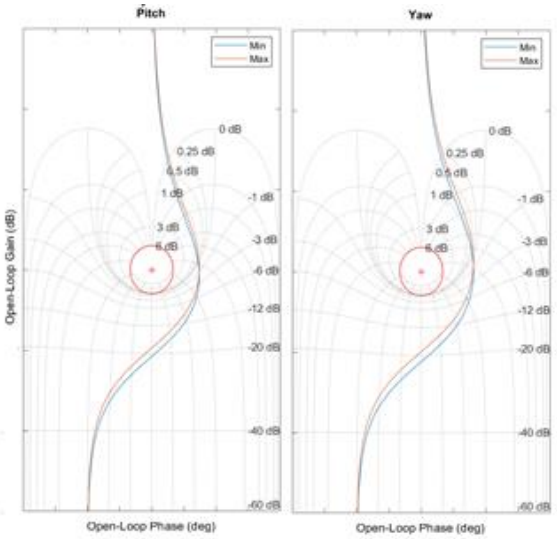

Figure 37. Updated RCS Pitch & Yaw Stability

11. ASSEMBLY, INTEGRATION, & TESTING

A number of Assembly, Integration, and Testing (AI&T) activities are necessary for the development of the MAV flight unit. Although these activities typically do not occur until fairly late in the project lifecycle of a launch vehicle, it is extremely important that preliminary planning of them is completed. This involves preparation of plans for assembly of the integrated vehicle from subsystem components, integration with external elements, verification and validation, and the development of a concept for an Earth-based flight test program. In support of these activities, four individual types of MAV units are planned: an Engineering Model (EM) unit, a Flight Test (FT) unit, an Assembly, Test, and Launch Operations (ATLO) unit, and a Flight Mission (FM) unit.

The EM unit is identical to the actual flight unit that will launch from Mars, except that it will have inert ordnances and pyrotechnics. This unit will be used for qualification testing of the MAV design. Parts of this unit, specifically the inert solid rocket motors, will also be used to support the higher-level ATLO tests without the need for facility safety requirements.

The FT unit will be used for an Earth-based flight test program. Multiple flight tests (two with an optional third) are planned. The flight test program will be used for validation of the integrated MAV second stage design. It is expected that the FT unit will be as similar to the MAV second stage as possible, including the separation system, live ordnances, and pyrotechnics. It will also have onboard development flight instrumentation, specific to the Earth-based flight test, used to collect engineering data. The FT unit will not be used for verification of MAV requirements. The FT unit is detailed further later in this section.

The ATLO unit is composed of a combination of EM and FM hardware. The ATLO unit contains flight mission avionics hardware and, ideally, as much of the other flight mission hardware as possible. It will not contain any live ordnances or pyrotechnics. Acceptance testing will be performed on the ATLO unit for actual flight hardware and software. Following completion of ATLO testing, the flight hardware components will be reintegrated with the live flight mission motors and pyrotechnics and integrated with the SRL S/C.

The FM unit is the actual unit traveling to and lifting off from Mars. The flight avionics from the ATLO unit are combined with live ordnance and pyrotechnics to make the FM unit.

Vehicle Assembly & Integration

Planning for the assembly of each unit begins at a subsystem component level. Following procurement, or, where applicable, in-house development and fabrication, individual hardware components will be installed on vehicle primary and secondary structures. Each stage will then be assembled in parallel, before integrating the stages into the full vehicle. The EM unit and FM unit will be developed in parallel. Following initial assembly and testing of the EM, the FM interstage and forward structure components will be removed and integrated into the EM. This will form the ATLO unit, which will include actual flight avionics. The ATLO unit will go through a series of acceptance tests with the MLP before ultimately being disassembled, with the interstage and forward structure components being reintegrated with the FM propulsion components. This process will allow for acceptance testing of the avionics/SRL S/C interface without pyrotechnic safety concerns. The assembly and integration process for the EM, FM, and ATLO units are summarized in Figure 38. Note that for the illustration, the EM unit and its respective hardware is shown in green as the MAS-EM, the FM and its respective hardware is shown in blue as the MAS-FM, and ATLO unit is shown in tan as the MAS-ATLO. The FT unit is not displayed.

Vehicle Testing

During the SRC, an initial plan for vehicle testing was established. This test plan includes a series of subsystem ground-based qualification and acceptance tests, as well as the aforementioned Earth-based integrated flight test. The MAV qualification test program will sequentially test component parts of the EM unit through each higher assembly, including both functional and environmental testing of all hardware. The intent is to eliminate design and manufacturing risk at the lowest assembly level possible within the bounds of a “test as you fly and fly as you test” methodology. The EM unit is planned to undergo functional and environmental qualification testing associated with grounding, altitude, leak, thermal vacuum/fatigue, acoustic noise, random vibration, shock, electromagnetic interference, mass properties, and spin balance testing. The FM unit would be limited in acceptance testing due to the presence of live propellant but would test to mission limits where applicable. Many cases will require specific test articles to be developed. A sample test article is shown in Figure 39, which would allow environmental testing of the entire integrated vehicle.

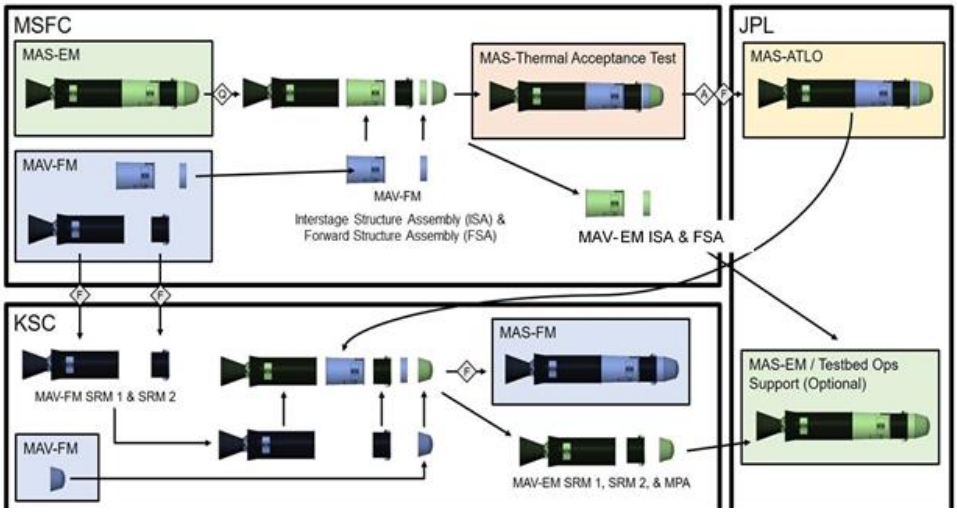

Figure 38. Assembly and Integration of MAV EM, FM, and ATLO Units

Three individual ground-based static firing tests are planned for each SRM. This will include testing of TVC units where applicable for SRM1. Aside from providing valuable validation of propulsive element designs, these tests will anchor the expected SRM performance in simulated Martian environments. Two of the tests are planned to use the same propellant batches as those in the FM, allowing for significant reduction in technical uncertainty of the actual flight motors.

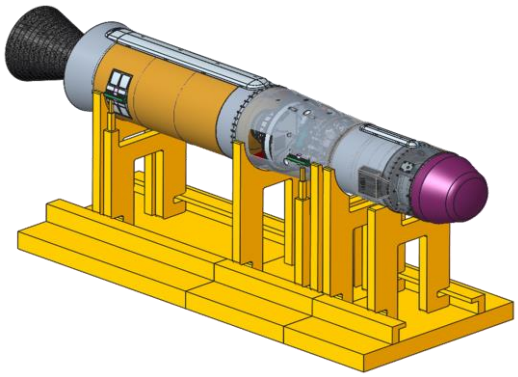

Figure 39. Notional Qualification Test Article

Some components of the MAV design, such as flight software, do not rely on actual physical testing. In cases such as this, a SIL is planned. This will allow all MAV stakeholders to conduct integration testing between software and hardware, confirming GN&C algorithms, running mission simulations, and performing off-nominal and fault insertion tests between subsystems.

Flight Test Planning

Given the lack of heritage of the MAV mission and its importance in the overall MSR campaign, the need for a flight test was identified prior to the beginning of the SRC. This was necessary to reduce overall technical risk and validate various systems in an integrated flight-like environment. Original feasibility concepts assessed the technical and programmatic capability of launching an Earth-based flight test vehicle from an altitude where atmospheric pressure would be similar to that of Mars. These early concepts featured the use of a high-altitude balloon with an attached MAV launch carrier. As these concepts gained fidelity, however, it was recognized that there would be a large cost associated with only a singular flight test with a lot of room for error. Additional developments of the MAV architecture from an SSGG to an SSGU configuration showed that a simpler overall test scheme would be a more effective use of resources. As part of the SRC a new concept of a sounding rocket-based flight test program was developed.

The concept for this updated flight test program involves placing the MAV second stage and portions of the first stage as a payload on an Earth-based sounding rocket. The FT unit would contain a stage 1 mass simulator and modified interstage. The interstage would have a non-flight-like attitude control system and avionics hardware to provide the same functionality of the actual MAV. The FT stage separation mechanism and second stage would be as similar to the actual MAV flight unit as possible. Although it would be ideal to test an entire integrated flight-like MAV, a large amount of uncertainty stems from the operation of the unguided second stage and its associated components. The first stage components, however, feature traditional configurations that can adequately be tested on the ground.

The flight test program itself is a risk reduction effort aiming to validate the integrated MAV design in environments that cannot be replicated with ground testing. Three primary flight test objectives are planned to be recognized. The first objective would be to reduce SRM2 performance uncertainty in an accelerating environment. Without flight data, vehicle performance must be modeled using a large uncertainty distribution. The second objective would be to characterize second stage integrated dynamics. Several factors contribute to overall system performance, such as impulse error and slag retention. The individual effects of these factors are difficult and, in some cases, impossible to characterize analytically. The third objective would be to demonstrate that the separation system performs its functions. Second stage spin-up effects on the separation system are impractical to achieve

through ground testing and do not have heritage in MAV mission environments. Aside from these primary objectives, a series of optional secondary objectives could also be performed based upon risk reduction, cost value, and instrumentation needs

Two individual flight tests are planned with a third option available as a backup in the event of unexpected failure. Each flight would begin with the MAV flight test unit being thermally conditioned to simulate Martian temperatures. The sounding rocket would then launch with onboard sensors to measure loads, acoustics, and dynamics in order to understand the health of the FT unit prior to separation. Once the target altitude has been reached, the MAV FT unit would separate, with data collected during separation from both stages for comparison. As with the actual flight unit, the second stage would spin up, ignite SRM2, then spin down following engine burnout. This will be when the bulk of data would be collected. During the entire test, ground stations would be used for tracking and gathering of telemetry. A concept of how the actual MAV flight test unit would fit within a sound rocket is shown in Figure 40. In this rendition, a Wallops Flight Facility Black Brandt IX sounding rocket is displayed, however, the actual sounding rocket may vary.

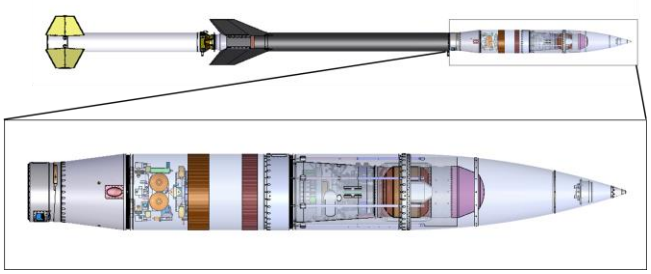

Figure 40. MAV FT Unit Stored Within Rocket

12. SUMMARY

The SRC configuration of MAV was found to successfully deliver a 16kg payload of 30 sample tubes to Martian orbit. To accommodate campaign direction to increase mass and volume margins, the vehicle architecture was updated to include an unguided, spin-stabilized second stage. A significant portion of avionics and RCS subsystem hardware has been moved to the first stage, reducing GLOM at the expense of orbit insertion accuracy. Mission design constraints were met under nominal conditions. The target orbit was achieved with most 6DOF dispersions, however, some cases were found to exceed the design constraint limits in various subsystems. As the vehicle design matures, these exceedances will be minimized.

13. ACKNOWLEDGEMENTS

The authors would like to thank the entire MAV team for their ongoing dedication and work on the MAV project through SRC and beyond. Without their extreme dedication to detail, engineering expertise, and lengthy documentation, this publication would not be possible.

14. REFERENCES

[1] NASA Procedural Requirements (NPR) 8704.1

[2] D. Yaghoubi, A. Schnell, "Mars Ascent Vehicle Solid Propulsion Configuration," *IEEE Aerospace Conference, March 2020*

[3] D. Yaghoubi, A. Schnell, "Mars Ascent Vehicle Hybrid Propulsion Configuration," *IEEE Aerospace Conference, March 2020*

[4] D. Yaghoubi, P. Ma, "Integrated Design Results for the MSR DAC-0.0 Mars Ascent Vehicle," *IEEE Aerospace Conference, March 2021*

[5] Aerojet Rocketdyne In-Space Propulsion Datasheets: Monopropellant and Bipropellant Engines, April 2020. https://www.rocket.com/sites/default/files/documents/In-Space%20Data%20Sheets%204.8.20.pdf

[6] S. Go, S. Lawrence, D. Mathias, R. Powell, "Mission Success of U.S. Launch Vehicle Flights from a Propulsion Stage-Based Perspective: 1980-2015" NASA TM-2017-219497, 2017.

[7] R. Hall, S. Hough, C. Orphee, K. Clements, "Design and Stability of an On-Orbit Attitude Control System Using Reaction Control Thrusters," *AIAA Guidance, Navigation, and Control Conference, January 2016*

15. BIOGRAPHY

Darius Yaghoubi *received a B.S. in Aerospace Engineering from North Carolina State University in Raleigh, NC in 2007. He has worked at NASA MSFC for 15 years. He has been a member of the MAV team since February 2018, initially starting as the GNC lead and transitioning to the vehicle technical lead in October 2018. He now works as the MAV Alternate Lead Systems Engineer and Integrated Analysis Team Lead. Prior to joining the MAV team, he worked as the lead pogo stability analyst on the NASA SLS program and supported separation and liftoff analysis on the NASA Ares program. He has also supported NASA groups in loads and dynamics, software integration, engineering testing, 3D printing, and deep space habitat. Aside from his technical work, Darius is an active member of the MSFC Speaker's Bureau and has represented NASA at a number of public outreach and speaking events.*

Shawn Maynor *has worked at NASA MSFC after receiving a B.S in Electrical Engineering from the University of Kentucky in Lexington, KY in 2012. He has worked Mission and Fault Management for SLS, NEA Scout, and MAV. He served as the M&FM lead for MAV from Spring 2019 until transitioning to a Technical Integration sub-lead role for the MAV Systems Engineering team in Summer 2021. He has also performed a developmental detail to certify as an operations controller in support of ISS payload operations conducted out of MSFC's Huntsville Operations Support Center.*